Molecular Therapy
Original Article

Systemic Injection of *RPE65*-Programmed Bone Marrow-Derived Cells Prevents Progression of Chronic Retinal Degeneration

Xiaoping Qi,[1] S. Louise Pay,[1,2] Yuanqing Yan,[3] James Thomas, Jr.,[4] Alfred S. Lewin,[4] Lung-Ji Chang,[4] Maria B. Grant,[1] and Michael E. Boulton[1]

[1]Department of Ophthalmology, Eugene and Marilyn Glick Eye Institute, Indiana University School of Medicine, Indianapolis, IN 46202, USA; [2]Department of Medical and Molecular Genetics, Indiana University School of Medicine, Indianapolis, IN 46202, USA; [3]Department of Pharmacology and Therapeutics, University of Florida, Gainesville, FL 32610, USA; [4]Department of Molecular Genetics and Microbiology, University of Florida, Gainesville, FL 32610, USA

Bone marrow stem and progenitor cells can differentiate into a range of non-hematopoietic cell types, including retinal pigment epithelium (RPE)-like cells. In this study, we programmed bone marrow-derived cells (BMDCs) ex vivo by inserting a stable *RPE65* transgene using a lentiviral vector. We tested the efficacy of systemically administered *RPE65*-programmed BMDCs to prevent visual loss in the superoxide dismutase 2 knockdown (*Sod2* KD) mouse model of age-related macular degeneration. Here, we present evidence that these *RPE65*-programmed BMDCs are recruited to the subretinal space, where they repopulate the RPE layer, preserve the photoreceptor layer, retain the thickness of the neural retina, reduce lipofuscin granule formation, and suppress microgliosis. Importantly, electroretinography and optokinetic response tests confirmed that visual function was significantly improved. Mice treated with non-modified BMDCs or BMDCs pre-programmed with *LacZ* did not exhibit significant improvement in visual deficit. *RPE65*-BMDC administration was most effective in early disease, when visual function and retinal morphology returned to near normal, and less effective in late-stage disease. This experimental paradigm offers a minimally invasive cellular therapy that can be given systemically overcoming the need for invasive ocular surgery and offering the potential to arrest progression in early AMD and other RPE-based diseases.

INTRODUCTION

Systemic delivery of an adult cell population that has the ability to home to dysfunctional tissue and differentiate into the correct cell type would be a major advance in therapeutic intervention for chronic degenerative diseases. Hematopoietic stem cells and progenitor cells offer such an approach because they are an endogenous source of stem and progenitor cells, freely circulating throughout the body, and are easily removed and re-administered.[1,2] These bone marrow-derived cells (BMDCs) can be used for autologous transplantation and can be delivered to the systemic circulation via intravenous injection, which is minimally invasive. Furthermore, BMDCs offer a population of cells that can be manipulated ex vivo and have a >30-year history of established efficacy and safety in humans, as shown by bone marrow transplantation.[1,2] Additionally, more than 362 clinical trials using bone marrow (BM)-derived cells have been registered with https://ClinicalTrials.gov, many of which have shown efficacy in at least one clinical endpoint.

It is now well recognized that adult bone marrow-derived stem and progenitor cells are not as lineage restricted as previously thought[3] and have the capacity to differentiate into a number of non-hematopoietic cells, for example, in the heart (cardiomyocytes, vascular smooth muscle cells, and myocardium),[4–6] liver,[7–9] pancreas,[10] muscle,[11,12] and CNS (e.g., microglia and macroglia, oligodendrocytes, neurons).[13–15] The eye is no exception, and we and others have shown that BMDCs have the capacity to differentiate into vascular endothelial cells, pericytes, astrocytes, microglia, and retinal pigment epithelial (RPE) cells.[16–19] Although these events are relatively rare, they occur in sufficient frequency to be detected by immunohistochemistry and can affect the physiology of the tissue. It has been proposed that this plasticity represents an underlying reparative process in response to tissue damage, and it is recognized that BMDCs are recruited to sites of injury. However, the low level of differentiation of BMDCs into non-hematopoietic lineages, even in the presence of an acute injury, has rendered BMDCs of limited value for regenerative medicine in the clinical setting. To address this, we have previously reported that BMDCs can be programmed ex vivo using a lentiviral vector to insert a stable *RPE65* transgene, which encodes a protein specific to RPE cell, to enhance differentiation to an RPE-like phenotype.[20] We demonstrated that systemic delivery of these programmed BMDCs in an acute mouse model involving chemical ablation of the RPE cell layer regenerated an efficient and functional RPE layer that, importantly, restored visual function in these animals.

Received 7 October 2016; accepted 6 January 2017;
http://dx.doi.org/10.1016/j.ymthe.2017.01.015.

Correspondence: Michael E. Boulton, Department of Ophthalmology, Indiana University School of Medicine, 980 Walnut Street, R3-426A, Indianapolis, IN 46202, USA.
E-mail: mboulton@iupui.edu

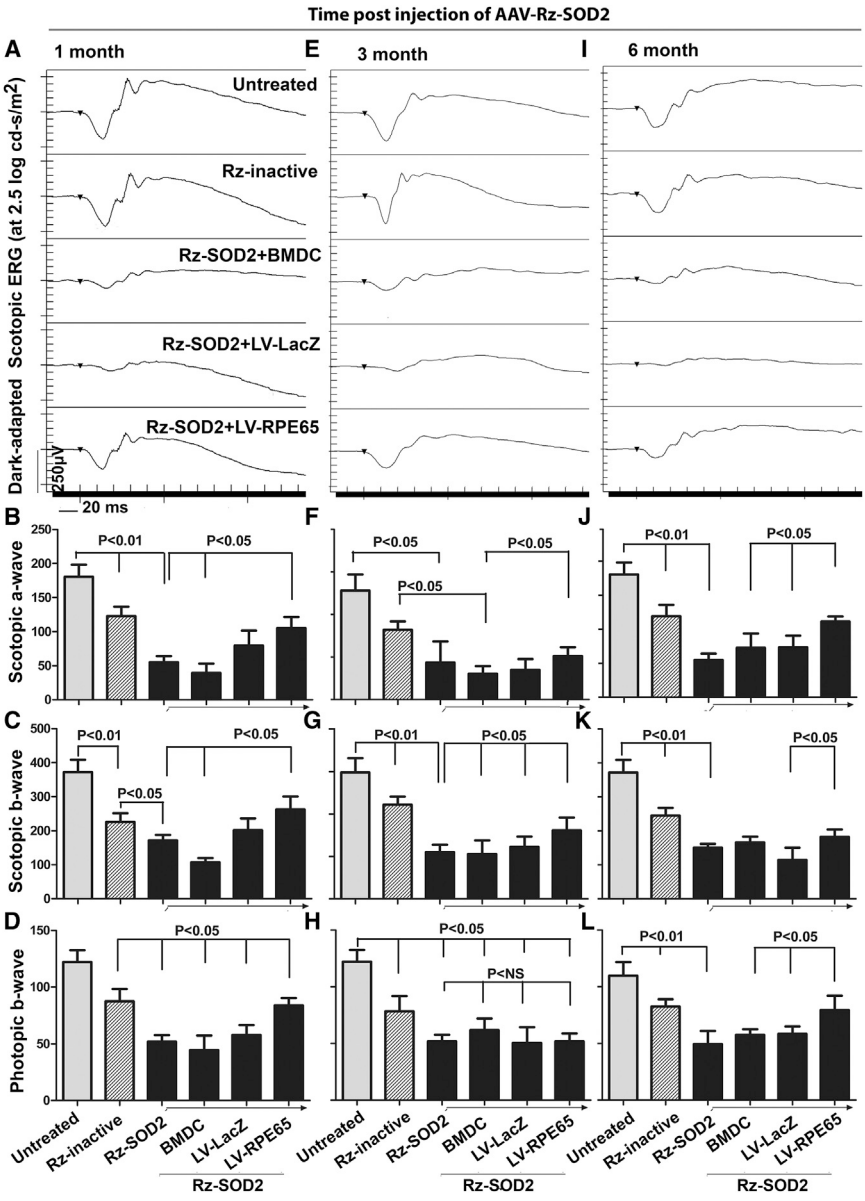

Figure 1. ERG Analysis Demonstrates Recovery of Response to Flash Stimuli in SOD2-KD Mice Treated with *RPE65*-Programmed BMDCs

C57BL6/J mice received subretinal injection of *AAV1-Rz-SOD2* or *AAV1-Rz-inactive* for 1, 3, or 6 months prior to tail vein injections of naive BMDCs, LacZ-programmed BMDCs (LV-LacZ), or RPE65-programmed BMDCs (LV-RPE65). Scotopic full-field electroretinograms and photopic electroretinograms were measured 3 months after systemic delivery of BMDCs. Representative ERG wave forms from dark-adapted mice in response to flashes of intense white light (2.5 log cd-s/m^2) are shown. (A, E, and I) The typical average maximum a and b wave ERG traces are shown for untreated normal, *AAV1-Rz-Inactive*-treated mice, and SOD2-KD animals after receiving naive BMDCs, LV-LacZ, or LV-RPE65. Scotopic a and b wave of mice treated 1 month (B and C), 3 months (F and G), and 6 months (J and K) post-SOD2-KD. Units on the y-axes are microvolts. (F and G) Scotopic a and b wave of mice treated 3 months post-SOD2-KD. Photopic b wave of mice treated 1 month (D), 3 months (H), and 6 months (L) post-SOD2-KD. Values are expressed as mean ± SEM.

Because RPE atrophy is a hallmark of age-related macular degeneration (AMD), a leading cause of chronic visual loss in the elderly,[21] we now sought to determine if *RPE65*-programmed BMDCs could prevent or slow the progression in a *Sod2* knockdown animal model that exhibits a chronic, progressive pathology with many of the features of AMD.[22,23] In this model, an adeno-associated virus (AAV) expressing a ribozyme that targets the protective enzyme manganese superoxide dismutase is injected beneath the retinas of adult mice. Pathology includes morphologic changes in the RPE and Bruch's membrane, accumulation of oxidatively modified proteins, increased levels of lipofuscin, RPE cell loss, and photoreceptor degeneration.[22,23] These are all hallmarks of AMD.[24,25] In this study, we were able to demonstrate that systemically administered, *RPE65*-programmed BMDCs localize to the subretinal space, repopulate the RPE layer, and restore visual function, and this regeneration was most effective if BMDC administration occurred early in the progression of disease.

RESULTS

RPE65-Programmed BMDCs Ex Vivo

Prior to investigating the capacity of RPE65-programmed BMDCs to repopulate the RPE in the SOD2-KD model, we verified, using a GFP-expressing control virus, that the lentiviral vector used was capable of infecting BMDCs with an efficiency of approximately 80% (Figures S1A and S1B). As we previously reported, this results in an average SOD2 reduction of 50% compared with inactive ribozyme control.[22] We confirmed that transduction with the RPE65 lentiviral vector induced expression of RPE65 within 24 hr and, additionally, CRALBP, a marker of RPE cells and Muller glia (Figures S1C–S1E).

RPE65-Programmed BMDCs Restore Visual Function in the *Sod2*-Knockdown Mouse Model

By 1 month following *Sod2* knockdown in the RPE, mice demonstrated a significant loss of electroretinography (ERG) response, at more than 75% ($p < 0.01$), compared with untreated animals, while, animals receiving the inactive ribozyme demonstrated a robust ERG response with strong a and b waves (Figure 1). This decreased ERG response was maintained out to 6 months following *Sod2* knockdown (Figure 1). Mice that received systemic RPE65-programmed

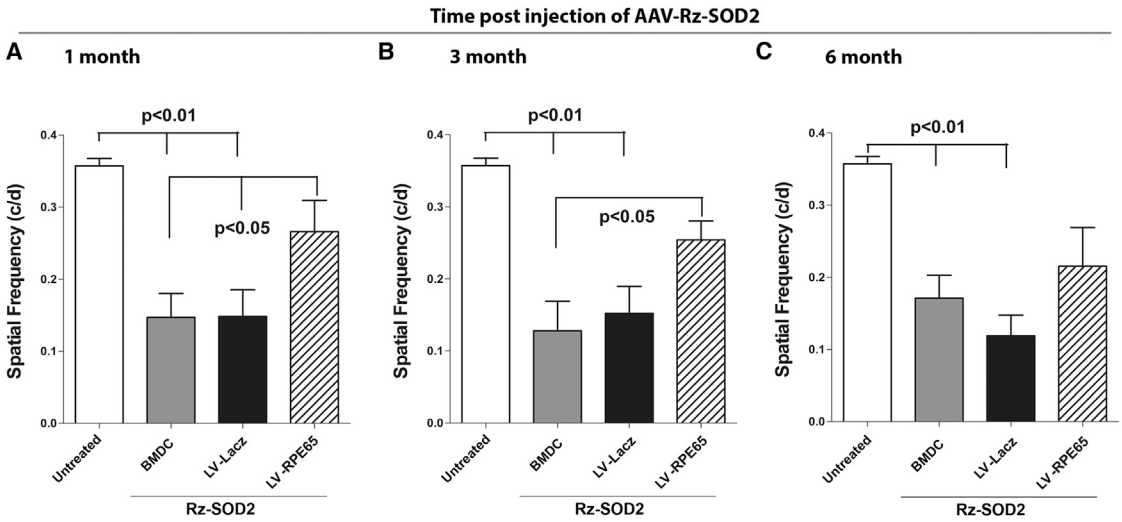

Figure 2. Visual Acuity Testing Demonstrates Recovery of Optokinetic Response in SOD2-KD Mice Treated with *RPE65*-Programmed BMDCs

C57BL6/J mice received subretinal injection of AAV1-Rz-SOD2 or AAV1-Rz-inactive for 1, 3, or 6 months prior to tail vein injections of naive BMDCs, LV-LacZ, or LV-RPE65. Spatial frequency thresholds were calculated 3 months after systemic delivery of BMDCs using an Optomotor behavioral test of optokinetic response. (A–C) A comparison of average values for photopic activities in response to rotating sinusoidal gratings is shown for each group of mice (n = 5 per group) treated with cells (A) 1 month, (B) 3 months, and (C) 6 months following SOD2 knockdown. Values are expressed as the mean ± SEM.

BMDCs 1 month after *Sod2* knockdown (early-stage degeneration) demonstrated significant recovery of ERG response, which was manifest in both the photopic and scotopic ERG (Figures 1A–1D). Such recovery was not observed in *Sod2*-knockdown mice receiving naive BMDCs or LacZ-programmed BMDCs. Mice that received systemic RPE65-programmed BMDCs 6 months after Sod2 knockdown (late-stage degeneration) demonstrated a modest but significant recovery in ERG response (Figures 1I–1L) compared with mice receiving naive BMDCs or LacZ-programmed BMDCs. Animals receiving RPE65-programmed BMDCs 3 months after *Sod2* knockdown showed an intermediate ERG response between the 1- and 6-month groups (Figures 1E–1H).

Although ERG is a gold standard for monitoring electrical activity in the retina, optokinetic response is commonly used in parallel, as it confirms that the animals can actually see a moving target, in this case a rotating grating. Whereas full-field ERG averages the electrical responses of the whole retina, rescue of vision in part of the retina will be detected by the optokinetic response. The spatial frequency of head turning was greatly reduced at all time points following *Sod2* knockdown compared with control mice (Figure 2). However, a significant improvement (>60%, $p < 0.05$) in optokinetic response was observed in animals receiving systemic RPE65-programmed BMDCs at both 1 and 3 months after *Sod2* knockdown (Figures 2A and 2B). No improvement was observed in animals receiving systemic naive BMDCs or LacZ-programmed BMDCs. No significant improvement was observed in animals receiving RPE65-programmed BMDCs at 6 months after *Sod2* knockdown (Figure 2C). Collectively, these data indicate that treating early in disease is likely to result in better recovery than treating at late stages, which is current clinical practice in RPE transplantation studies.

RPE65-Programmed BMDCs Integrate into the RPE Layer of Sod2-Knockdown Mice

We have previously confirmed that RPE65-programmed BMDCs are recruited from the circulation and can restore the RPE layer in mice pretreated with $NaIO_3$ to ablate the RPE layer.[20] Both RPE flat mounts and retinal cross sections demonstrated GFP^+ RPE65-BMDCs integrating into the existing RPE monolayer by 3 months after injection into the Sod2 knockdown model (Figure 3). These GFP^+ cells incorporated either as individual cells or as small areas of three to seven cells and stained positive for both RPE65 and CRALBP, both specific markers of RPE cells. We did not observe GFP^+ cells elsewhere in the neural retina or choroid at the time points studied. Additionally, although we initially observed significant GFP expression in the spleen, we did not observe significant expression of GFP in the lung, spleen, or bone marrow of mice injected with BMDCs treated with TYF-RPE65 (a lentiviral vector expressing RPE65) by 28 days after injection (Figure S2). Mice receiving BMDCs transduced with a control lentivirus vector (TYF-LacZ) did not demonstrate a significant signal (data not shown).

Evaluation of the integrity of the RPE layer was determined by immunostaining RPE flat mounts for the tight junction protein ZO-1 (Figure 4A). ZO-1 demonstrated strong staining of the RPE lateral cell membranes and excellent RPE integrity in normal untreated eyes. However, RPE flat mounts from SOD2-knockdown animals that received no BMDCs (data not shown) or LacZ-programmed BMDCs showed weak ZO1 staining and a disorganized RPE layer with cell loss and background autofluorescence consistent with lipofuscin accumulation. By contrast, SOD2-knockdown animals that

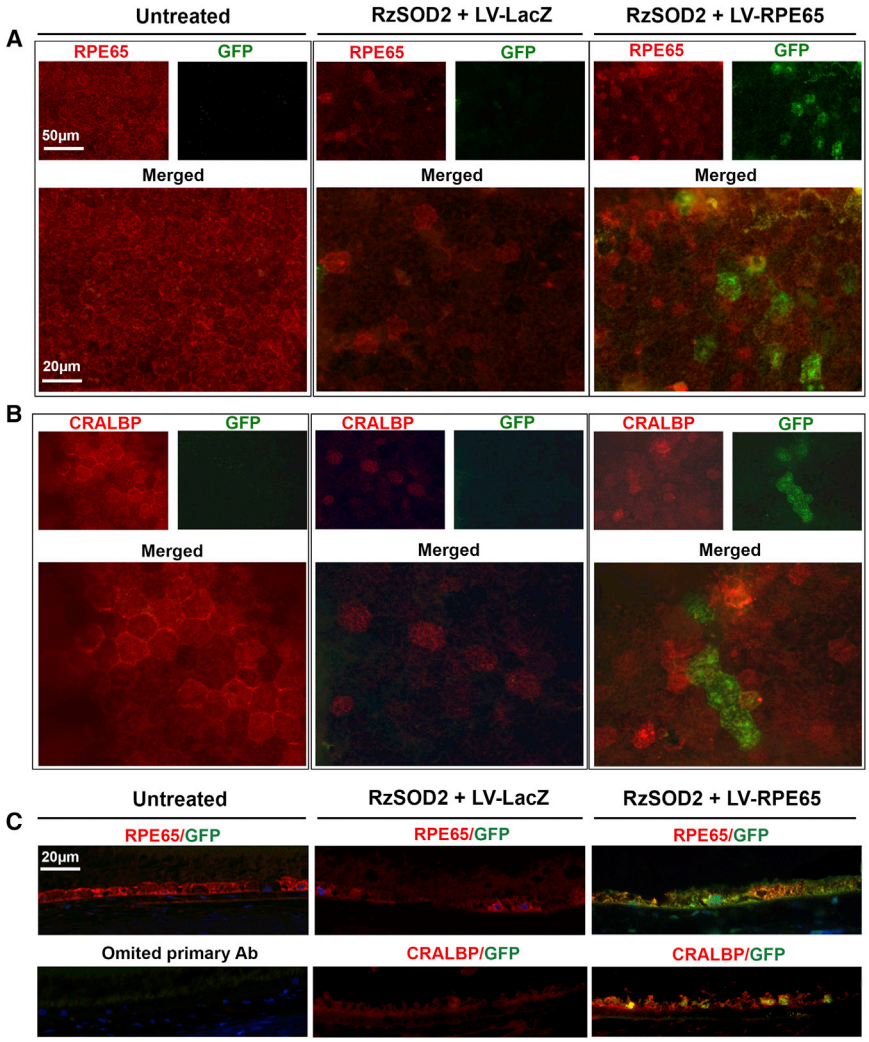

Figure 3. GFP⁺ BMDCs Expressing RPE65 Colocalize with the Host RPE and Express RPE Markers

One month after SOD2-KD, animals were treated systemically with naive BMDCs, LacZ-programmed BMDC, or RPE65-programmed BMDCs. (A–C) Representative fluorescent micrographs of flat-mounted posterior cups RPE/choroid (A and B) and paraffin sections (C) were stained for RPE65 (red) (A), CRALBP (B) (red), and GFP (green) to demonstrate colocalization. Note the significantly greater presence of GFP⁺ cells in animals receiving RPE65-programmed BMDCs. The cross-section of the RPE in (C) shows colocalized green (GFP⁺) and red (RPE65 or CRALBP⁺) cells at the RPE layer. Note the percentage of GFP⁺ cells that are mature and express CRALBP is much higher in the animals receiving RPE65-programmed BMDCs than in untreated control or LacZ-programmed BMDCs.

received RPE65-programmed BMDCs showed the typical ZO-1 staining of the host RPE lateral cell membranes, good RPE morphology, and minimal background autofluorescence. GFP-positive RPE65-programmed RPE cells are clearly seen inserted in the host RPE layer and show ZO-1 staining at their later membranes (Figure 4A). On average, between 65% and 85% of the whole RPE flat mount shows GFP⁺ cells, and this RPE cell density is highest in the nasal quadrants closest to the subretinal injection site. Analysis of the number of BMDCs taken between 0.2 and 1.2 mm adjacent to the optic nerve head showed that up to 25% of the total RPE population consisted of GFP⁺ cells in animals receiving RPE65-programmed BMDCs, whereas this value was only about 1% for LacZ-BMDC (Figure 4B). We previously showed in a different model that RPE65-programmed BMDCs, once established on Bruch's membrane, are capable of photoreceptor outer segment phagocytosis.[20] Immunostaining demonstrates rhodopsin-positive phagosomes within the RPE of both host and GFP⁺ donor cells (Figures 4C and 4D).

RPE65-Programmed BMDCs Reduce Retinal Pathology in the *Sod2*-Knockdown Mouse Model

Pathology was similar to that reported by Justilien et al.[22] (Figure S3). One month after *Sod2* knockdown, the retinas began to exhibit loss of pigmentation in the RPE. The neural retina appeared relatively normal at this stage, although some disorganization of the inner and outer photoreceptor segments could be observed. At 3 months following *Sod2* knockdown, more pronounced changes to the RPE, such as vacuole formation and atrophy, were observed, together with shortening and disorganization of the outer and inner segments of the photoreceptors (Figure S3), and this became progressively more severe by 6 and 9 months following *Sod2* knockdown. Mice treated with control naive BMDCs or BMDC-LacZ demonstrated similar progressive pathology to that of untreated *Sod2*-knockdown mice, irrespective of the time administered following *Sod2* knockdown (Figures 5A–5C). In contrast, mice receiving RPE65-programmed BMDCs demonstrated a mature, highly pigmented epithelial layer with RPE morphology consistent with the normal controls across all time points of systemic administration following Sod2 knockdown (Figures 5A and 5C, insets). Furthermore, the morphology of the neural retina was greatly improved in animals receiving RPE65-programmed BMDCs compared with controls. Reduced thinning of both the inner and outer retina was observed in mice treated with RPE65-programmed BMDCs at 1, 3, and 6 months after *Sod2* knockdown (Figures 5 and S4). Preservation of the photoreceptor layer and inner retina was most pronounced when mice were treated 1 month after *Sod2* knockdown and was comparable with that of a normal eye. However, as can be seen in Figures 5C and S4F, when RPE65-programmed BMDCs were administered after the disease phenotype had fully

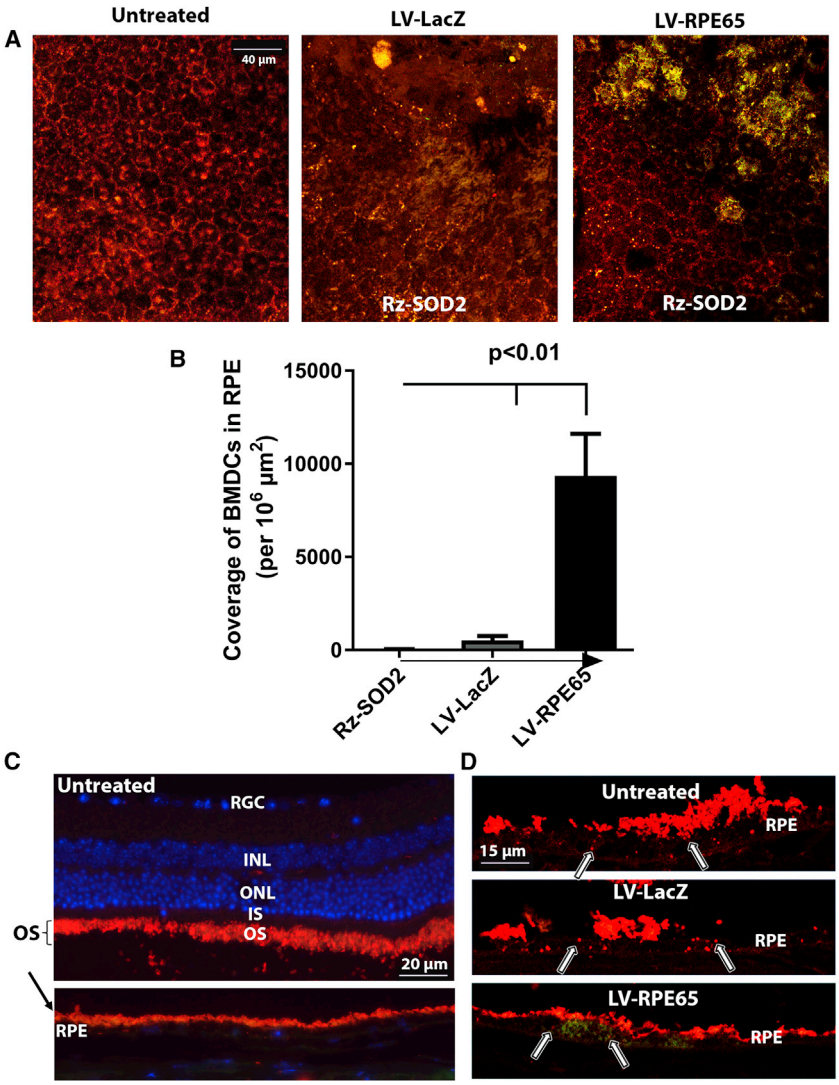

Figure 4. RPE65-Programmed BMDCs Enhance Host RPE Morphology and Phagocytose Photoreceptor Outer Segments

Representative photomicrographs are from animals that received subretinal AAV1-Rz SOD2 for 1 month and were then treated systemically with null BMDCs, LacZ-BMDCs, or RPE65-programmed BMDCs. Eyes were assessed 3 months later. (A) Immunostaining for the tight junction protein, ZO-1 (red), and co-distribution with BMDC-GFP$^+$ cells in RPE flat mounts from normal untreated animals and SOD2-knockdown animals that received either LacZ- or RPE65-programmed GFP$^+$ BMDCs (green). Animals receiving RPE65-programmed BMDCs showed the typical ZO-1 staining of the host RPE lateral cell membranes, while the RPE was disorganized, compared with control, in animals receiving LacZ-programmed BMDCs. (B) Quantification of BMDC-GFP$^+$ cells per unit area of a RPE flat mount taken between 0.2 and 1.2 mm adjacent to the optic nerve head. Up to 25% of the total RPE population consisted of GFP$^+$ cells in animals receiving RPE65-programmed BMDCs, whereas this value was only about 1% for LacZ-BMDCs (mean ± SEM). (C) Immunostaining for rhodopsin in retinal tissue sections from untreated animals showing intense rhodopsin staining in the photoreceptor outer segments above the RPE and in phagosomes within the RPE. (D) High-magnification photomicrographs of the RPE from untreated animals and SOD2-knockdown animals that received either LacZ- or RPE65-programmed BMDCs showing phagosomes (red, arrows) both within the host RPE and in GFP$^+$ RPE65-programmed BMDCs that have localized to the RPE layer.

developed, although the RPE layer appeared to be restored to a near normal state, a significant reduction in the photoreceptor layer was not recovered by treatment with RPE65-programmed BMDCs. Overall these data highlight that (1) early intervention prevents disease progression, whereas late intervention in advanced diseases shows only modest retinal regeneration, and (2) despite considerable improvement in retinal morphology in late-stage disease, recovery of visual function was only minimal.

Accumulation of the autofluorescent age pigment lipofuscin in the RPE is a characteristic of aging and AMD,[26] and as we previously reported, lipofuscin accumulation is a key feature in the *Sod2*-knockdown model.[22,27] *Sod2* knockdown resulted in a 6-fold increase in autofluorescence by 6 months, which was reduced 2.6-fold by treatment with RPE65-programmed BMDCs but not naive BMDCs or LacZ-programmed BMDCs (Figures 6A and 6B). A second feature of AMD is the appearance of activated microglia in the subretinal space.[28,29] Here, we show in retinal flat mounts a significant numbers of Iba1$^+$ microglia 6 months after *Sod2* knockdown, and these Iba1$^+$ cells exhibited morphological characteristics of ramified and activated microglia (Figure 6C). Animals treated with RPE65-programmed BMDCs demonstrated a significant >2.5 fold reduction in Iba1$^+$ cells that was not observed in mice treated with either naive BMDCs or LacZ-programmed BMDCs (Figures 6C and 6D). Because SOD2 plays a vital role in cellular defense against oxidative damage we assessed 4-hydroxynonenal (4-HNE) in tissue sections. Immunohistochemistry demonstrated that RPE65-programmed BMDCs resulted in a reduction in 4HNE in the retina compared with mice receiving null BMDCs or LacZ-BMDCs (Figure 6E).

DISCUSSION

AMD is a leading cause of severe, irreversible central vision loss affecting more than 1.7 million Americans.[30] There are two forms of AMD: neovascular or "wet" AMD, which represents the most severe form of the disease and affects about 15% of patients with AMD and can be treated with anti-VEGF therapies, and the atrophic or "dry" form, which affects 85% of patients with AMD and for which there is currently no treatment. Advanced dry AMD is characterized

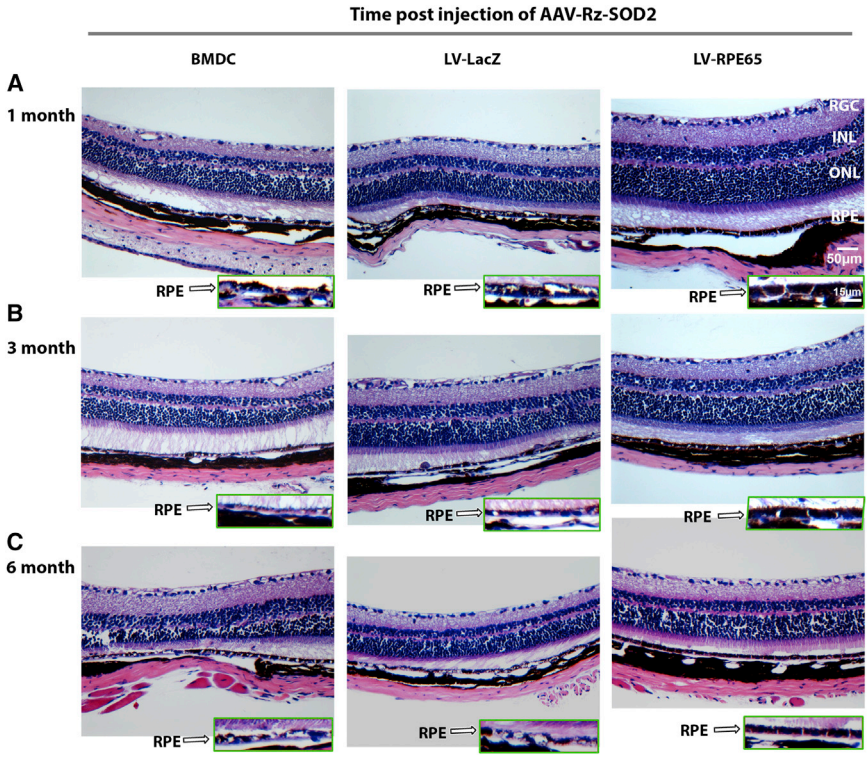

Figure 5. SOD2-KD Mice Treated with RPE65-Programmed BMDCs Show Improved Retinal Morphology

(A–C) C57BL6/J mice received subretinal injection of AAV1-Rz-SOD2 or AAV1-Rz-inactive 1 month (A), 3 months (B), or 6 months (C) prior to tail vein injections of naive BMDCs, LV-LacZ, or LV-RPE65. Histology was assessed 3 months after systemic delivery of BMDC. Photomicrographs are representative of 10 μM cross-sections of the retina/choroid/sclera stained with H&E. Inserts show higher power images of the RPE layer. It is evident that systemic administration of RPE65-programmed BMDCs shows normal retinal thickness and near normal RPE morphology, which is not apparent in eyes receiving either naive BMDCs or LV-LacZ. RGC, retinal ganglion cell layer; INL, inner nuclear layer; ONL, outer nuclear layer.

by geographic atrophy and loss of the RPE in the central retina, followed by subsequent degeneration of overlying photoreceptor cells. There is currently no reliable therapy for dry AMD. Two broad approaches, antioxidants and cellular therapy, have been used to address this major clinical problem. One established cell therapy involves RPE cell transplantation or replacement and represents a realistic strategy in the treatment of retinal degeneration,[31,32] as it involves one cell type and does not require the re-establishment of neural networks.

Both freshly isolated and cultured RPE cells have been transplanted into the subretinal space of animal models and AMD patients.[31–33] Although success has been observed in animal models with both integration of cells into the RPE layer and recovery of vision,[31,32] results have been limited in humans, with either a halt in progression or only one or two lines of improvement.[31,32] The poor outcomes have several explanations: (1) the invasive surgery required to prepare the subretinal space; (2) late-stage disease is associated with marked loss of RPE and photoreceptors; (3) a change in myeloid activation and glia activation in the aging retina, or (4) the source of RPE (i.e., advanced donor age).[31,34] To overcome some of these problems, human embryonic stem cells (hESCs) or induced pluripotent stem cell (iPSC)-derived RPE cells have been used for subretinal transplantation.[33,35,36] Studies have reported success with both hESC- and iPSC-derived RPE in restoring vision in animal models,[35,36] but although these RPE cell transplants in humans do not result in rejection or hyperproliferation, vision was not greatly enhanced post-transplantation.[35] Although extremely promising, concerns remain regarding genetic stability, and this approach does not overcome the necessity to invade the subretinal space or limitations in disseminating cells across the fundus. In 2015, an experimental study in Japan was halted because of unanticipated mutations accumulated in the iPSC-derived RPE cells (http://www.nature.com/nbt/journal/v33/n9/full/nbt0915-890.html). In general, however, transplantation of RPE cells has been safe, and that was the goal of the early-stage clinical trials. Perhaps most important, the requirement for subretinal administration of human ESC/iPSC-derived RPE will not easily overcome the ethical problems associated with using this approach to treat early AMD, when the microenvironment is less hostile and there is only minimal loss of overlying photoreceptors. Thus, our approach of systemic delivery of adult cells that have the ability to home to dysfunctional tissue (RPE) in early-stage AMD and to differentiate into the correct cell type represents a major advance in the early therapeutic intervention of this chronic vision threatening degenerative disease. Furthermore, the systemic approach is potentially more amenable to repeat treatments.

Here, in addition to confirming our previously published data showing that RPE65-programmed BMDCs are capable of repairing damaged RPE, protecting the photoreceptor layer, and retaining retinal thickness,[20] we have extended the model to include a closer representation of the pathophysiology of human dry AMD, the *Sod2*-KD model. We show that systemically administered RPE65-programmed BMDCs can traverse across the retina into an intact, albeit dysfunctional host RPE monolayer, either as individual cells or small clumps, and that this is sufficient to retain visual function, maintain the photoreceptor layer, preserve neural retina thickness, maintain phagocytosis of photoreceptor outer segments, reduce oxidative damage, suppress lipofuscin formation, and reduce microgliosis. It is not clear to what extent these beneficial effects are due to BMDCs' forming a functional RPE (we show ZO-1 staining and outer segment uptake), BMDCs' secreting neuroprotective factors (e.g., PEDF or neurotrophins),[37,38] or a combination of the two. Not

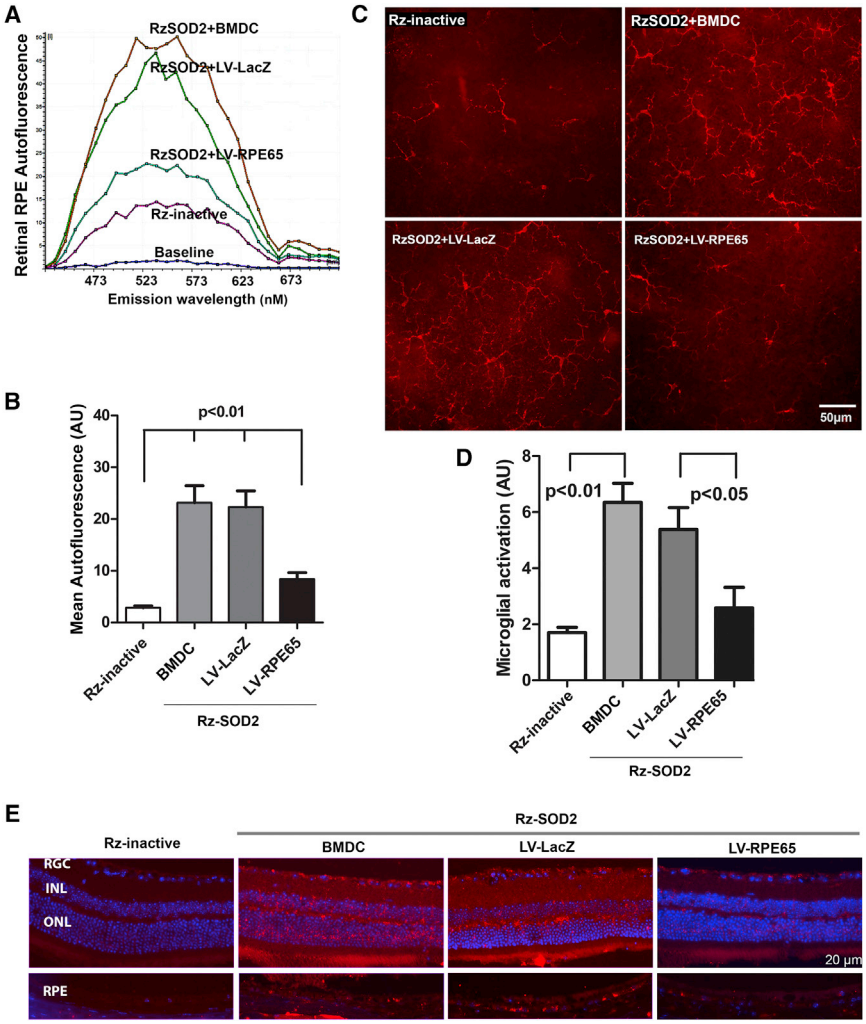

Figure 6. RPE65-Programmed BMDCs Reduce Lipofuscin Accumulation, Microglial Changes, and Oxidative Damage in SOD2-Knockdown Mice

C57BL6/J mice received subretinal injection of AAV1-Rz-SOD2 or AAV1-Rz-inactive for 1, 3, or 6 months prior to tail vein injections of naive BMDCs, LV-LacZ, or LV-RPE65. Lipofuscin accumulation and microglial changes were assessed 3 months after systemic delivery of BMDC. (A) Spectral profile study analyzed from lambda scan for autofluorescence. Mean peaks located at an emission wavelength of 523–573 nM. (B) Quantification of autofluorescence in the RPE layer by lambda scan showing a 6-fold induction of lipofuscin in the RPE of SOD2-knockdown animals and a >2-fold reduction of lipofuscin autofluorescence in the RPE of animals receiving RPE65-programmed BMDCs ($p < 0.05$; mean ± SEM; n = 5). (C) Representative confocal fluorescence micrographs from flat-mounted retina showing that the inactive Rz control retina contains just a few microglia that are scarcely distributed in the retina, while the retinas of SOD2-KD animals demonstrate a significant increase in the presence of microglia in the retina. This increase in retinal microglia staining was not suppressed in eyes treated with LacZ-programmed BMDCs but was greatly decreased in animals receiving RPE65-programmed BMDCs. (D) Quantitative analysis showed a 3-fold upregulation in microglia staining following SOD-KD, while animals treated with RPE65-programmed BMDCs showed a greater than 50% decrease in microglia compared with eyes treated with LacZ-programmed BMDCs ($p < 0.05$; mean ± SEM; n = 5). (E) Immunohistochemical detection of 4-HNE as a marker of oxidative stress 3 months after BMDC treatment. The representative photomicrographs show a low level of 4-HNE immunostaining (red) in the retinas of animals receiving inactive ribozyme alone, while SOD2-knockdown retinas showed a dramatic increase in 4-HNE staining that was not reduced by treatment with null BMPCs or LV-LacZ. However, 4-HNE staining was dramatically reduced in the retinas of SOD2-knockdown animals receiving RPE65-programmed BMDCs.

surprisingly, RPE65-programmed BMDC administration was most effective in early disease, with visual function and retinal morphology returning to near normal levels, and much less effective in late-stage disease, in which BMDCs were attempting to repair more severe pathology. Taken as a whole, our results suggest that RPE65-programmed BMDCs have a therapeutic effect on many aspects of dry AMD development. Naive BMDCs or BDMCs pre-programmed with *LacZ* did not exhibit significant improvement in visual deficit.

Two major concerns with regard to this type of systemic treatment are localization of BMDCs to other organs and the potential for cell fusion. The most likely localization of adoptively transferred BMDCs will be the lung, spleen, and bone marrow. However, by both 7 and 28 days following administration, GFP expression (sensitive to ten cells) was not significantly expressed in either lung or bone marrow. There was some localization to the spleen at 7 days, but this had declined to baseline at 28 days following administration. Animals receiving BMDCs did not demonstrate any systemic symptoms at any of the time points studied. Although our findings are promising, a number of studies have highlighted that apparent re-differentiation may result from cell fusion, leading to subsequent tissue regeneration following treatment, as opposed to true fate switching of the cells.[39–45] We have previously excluded the possibility of cell fusion, however, by the use of fluorescent in situ hybridization to support the absence of any BMDC fusion with host RPE,[20] and there is little doubt that BMDCs are recruited to sites of injury. In addition, it has been proposed that the bone marrow contains cells expressing early markers of non-hematopoietic cell types that are recruited to and promote regeneration of non-hematopoietic tissue types upon injury to that tissue.[6,11] Howell et al.[46] reported that cells termed "universal pluripotent stem cells" may be present in a number of tissues, including the brain and the blood, which have the ability to generate cell types of a different lineage from the tissue in which they reside under conditions which support such differentiation; that is, cellular differentiation

occurs when cells are in the correct microenvironment for the cell type they are capable of becoming.

As successful fate switching of adult stem cells is inextricably linked to the expression of markers present early in the development of the intended cell type, cellular transcriptional status, and microenvironment,[6,46,47], our one-step protocol is thought to be successful because of: (1) upregulation of a gene, *RPE65*, that is expressed in both early RPE development and in terminally differentiated RPE cells; (2) the fact that *RPE65* encodes a protein (all-trans-retinyl-ester hydrolase) that modulates retinoic acid, a transcriptional regulator and inducer of differentiation;[20] and (3) recruitment of the cells from the bloodstream to the vasculature of the eye. We propose that the local microenvironment in the eye "completes" the differentiation of BMDCs into fully functional RPE-like cells following RPE-layer infiltration and are currently investigating the role of *RPE65* in promoting RPE65-programmed BMDCs retention in the eye.

Given that expression of a single gene is capable of promoting differentiation of BMDCs into RPE-like cells, we believe that it may be possible to generate other cell types from BMDCs using a similar process. Photoreceptor specific genes could be used to enhance differentiation of progenitors capable of regenerating photoreceptors in addition to treating dry AMD or inherited retinal degenerations, for example. Alternatively, cell type-specific gene expression could be used to target other disorders involving tissue degeneration. Theoretically, it may be possible that any cell type could be generated from BMDCs by applying the principles used to select the *RPE65* gene, as long as the modified cell is recruited to the microenvironment correct for the target cell type in vivo. Attempting to generate tissue in a cell culture setting with modified BMDCs is perhaps not as likely to be successful if the cell must be in its natural microenvironment for the differentiation process to be finalized; therefore, modified BMDCs should perhaps be tested in vivo during the early stages of developing the modification strategy as opposed to characterizing cells in vitro as is typical of current iPSC technology. Indeed, we have never observed the generation of an RPE-like layer with RPE65-programed BMDCs in vitro, yet the cells are clearly capable of forming one in vivo.

In conclusion, we have shown that genetically modified BMDCs are recruited to sites of cellular dysfunction and are able to reverse pathology. Not surprisingly, prevention of pathology by administration at the early stages of disease was far more effective than administration of programed BMDCs in late stages of disease with severe pathology. Thus, modified BMDCs may provide an ideal therapy not only or AMD but also other degenerative diseases, provided the correct programming strategy can be identified.

MATERIALS AND METHODS

Materials

EasySep Mouse Hematopoietic Progenitor Cell Enrichment Kit and EasySep Mouse SCA1 Positive Selection Kit were purchased from STEMCELL Technologies. DMEM (high glucose) was purchased from Life Technologies. Polybrene and paraformaldehyde were ordered from Sigma-Aldrich. The antigen retrieval solution Rodent Decloaker 10× was purchased from Biocare Medical. For the antibodies, anti-RPE65 (catalog sc-73616) was from Santa Cruz Biotechnology; anti-CRALBP (MA1-813) was from Thermo Scientific; microglia detection antibody, anti-Iba1 (019-19741), polyclonal, rabbit was purchased from Wako Chemicals USA; and the secondary antibody with Alexa Fluor 594 (Z25007) was from Invitrogen. All sections were mounted with Vector Shield medium from Vector Laboratories.

Animals

All animal studies were conducted under protocols approved by the Institutional Animal Care and Use Committees at Indiana University and the University of Florida and in accordance with guidelines set forth by the National Institutes of Health and the Statement for the Use of Animals in Ophthalmic and Visual Research of the Association for Research in Vision and Ophthalmology. Adult (7- to 10-week-old) female C57BL/6J mice and homozygous GFP transgenic (C57BL/6-Tg [UBC-GFP]) were purchased from Jackson Laboratories. For ocular injections and electroretinography, mice were anesthetized by ketamine (72 mg/kg)/xylazine (4 mg/kg) intraperitoneal injection with topical anesthesia using proparacaine hydrochloride. Mice were euthanized by isoflurane in a desiccation chamber in the fume hood flowing by cervical dislocation.

Preparation of RPE65-Programmed BMDCs

We programmed BMDCs ex vivo by inserting a stable *RPE65* transgene using a lentiviral vector. In brief, $Lin^{-}Sca1^{+}$ BMDCs were isolated aseptically from bone marrow from tibiae and femurs of GFP^{+} mice according to our standard protocol[20] using EasySep Mouse Hematopoietic Progenitor Cell Enrichment Kit followed by EasySep Mouse Sca1 Positive Selection Kit. Lentiviral constructs expressing RPE65 (TYF-RPE65) and LacZ (TYF-EZ-LacZ) were prepared as previously described.[20] $Lin^{-}Sca1^{+}$ BMDCs were suspended in DMEM (high glucose), polybrene (8 μg/ml) plus 10% fetal bovine serum to a final cell concentration of 5×10^4 cells/mL. For the infection, the BMDCs were split into three 1×10^5 cell aliquots. Two aliquots were infected with 5 μL of recombinant lentivirus expressing TYF-EZ-LacZ or 2 μL of lentivirus expressing TYF-RPE65 respectively at a multiplicity of infection of ~50. The third aliquot received 5 μL of PBS (pH 7.4) as vehicle control. After washing and resuspension, cells were injected into mice as described below.

Subretinal Injection

C57BL/6J mice were anesthetized with a mixture of ketamine and xylazine; phenylephrine and a topical anesthetic were applied to the eyes. All procedures were performed under a Nikon high-resolution dissecting microscope. We used a 28-gauge blunt-tipped needle with bevel up to puncture the pars plana to make an opening into the vitreous cavity. Then, a 33-gauge blunt needle was inserted through the opening made into the vitreous chamber. Subsequently, the needle was angled to point slightly nasally and guided posteriorly into the eye toward the injection site. Upon penetration of the retina, 1 μL of sample with fluorescein mixture was slowly deposited

subretinally, and the small retinal bleb formed was visible with the green fluorescein located subretinally.

Generation of SOD2-Knockdown Mice

The right eyes of C57BL/6J mice were injected subretinally with 1 μL of 2.5×10^{12} particles/mL of recombinant AAV1 constructs on the basis of the pTR-UF2 vector expressing SOD2-specific hammerhead ribozyme, Rz432, driven by RPE-specific VMD2 promoter (*AAV1-Rz-SOD2*), to drive ribozyme gene expression efficiently in the RPE layer as previously described.[22] Control injections of rAAV-inactive ribozyme (*AAV1-Rz-inactive*) were performed in the right eyes of additional animals. The inactive ribozyme, although catalytically inert, retains sequence complementarity to Sod2 mRNA and thus may retain some limited antisense activity.

Systemic Administration of BMDCs

At 1, 3, and 6 months following SOD2-knockdown mice received a systemic injection of 5×10^4 $Lin^-Sca1^+GFP^+$ BMDCs (either naive BMDCs, BMDC-LacZ, or BMDC-RPE65) in 100 μL of sterile saline systemically administered into the tail vein (n = 5 per group). Negative controls included injection of the inactive ribozyme and untreated age-matched wild-type C57BL/6J mice.

Visual Function Tests

Two visual function tests were performed 3 months following injection of BMDCs: ERG and optokinetic nystagmus (OKN) response, as previously described.[29,48]

For ERG, mice were dark-adapted overnight, and full-field electroretinograms were recorded with a visual electrodiagnostic system (UTAS-E 2000; LKC Technologies) using gold wire loop electrodes placed on each cornea and a reference electrode placed subcutaneously between the eyes. Scotopic rod recordings were performed with stimuli presented at intensities of 0.025, 0.25, and 2.5 log cd-s/m^2 at 10, 20, and 30 s intervals, respectively. Ten responses were recorded and averaged at each light intensity. Photopic cone recordings were performed after mice were light-adapted to a white background light of 100 cd-s/m^2 for 5 min. Recordings were performed with four increasing flash intensities of 0, 5, 10, and 25 log cd-s/m^2 in the presence of a constant 100 mcd-s/m^2 rod suppressing background light. Fifty responses were recorded and averaged at each intensity. The a waves were measured from the baseline to the peak in the cornea-negative direction, and b waves were measured from the cornea-negative peak to the major cornea-positive peak. ERG data are presented as comparisons between treatment conditions for the mean of the maxima for a wave and b wave responses.

To evaluate the optokinetic response, we used a computer-based visual acuity response test (OptoMotry 1.7.7; Cerebral Mechanics). In brief, mice were tested for visual acuity by observing optokinetic responses of mice to rotating sinusoidal gratings.[48] Mice were placed on the platform and allowed to settle for 2 min. The virtual drum was rotated for 1 min, and the mice were observed for a head-tracking response. Initially, the 100% contrast pattern had a spatial frequency of 0.200 cycles/degree for both directions of rotation. The OptoMotry program changed spatial frequency on the basis of the observer's responses and tracked the responses according to direction of pattern rotation to assess the two eyes independently.

Immunohistochemical Analysis of RPE65 and CRALBP Protein Expression in BMDCs Ex Vivo

For immunohistochemistry, BMDCs-RPE65 and controls were cultured overnight at 37°C, and the following day, cells were washed with PBS and fixed in freshly prepared 4% paraformaldehyde. After three washes in PBS, cells were permeabilized with 0.1% Triton X-100 for 10 min at room temperature. Samples were then blocked by incubation with 5% normal goat serum in PBS for 1 hr at room temperature and incubated with mouse anti-RPE65 (1:200 in blocking solution) (Santa Cruz Biotechnology) and mouse anti-CRALBP (1:200) (Thermo Scientific) overnight at 4°C. Cells were then incubated with Alexa Fluor 594 goat anti-mouse IgG (1:600 in blocking solution) (Invitrogen) for 1 hr at room temperature. After extensive washing with PBS, cells were mounted with VectaShield DAPI (Vector Laboratories) for nuclear staining. Negative control samples were processed with the omission of the primary antibody. The cells were examined using an Axiovert 135 fluorescence microscope (Carl Zeiss) with identical settings for laser intensity, gain, and so on.

Flat-Mount RPE and Neural Retina Imaging

Eyes were enucleated and cleaned of fat and muscle, and the lens, vitreous, and cornea were carefully removed. Four shallow incisions were then made in the eyeball, allowing for separation of the retina from the RPE/choroid with minimal cross-contamination. The RPE/choroid was then flattened on a glass slide with the RPE facing upward and gently covered with a glass coverslip. The same procedure was carried out for the retina.

Quantitative RT-PCR for Localization of BMDCs in Different Tissues

C57BL6/J mice received 50,000 GFP^+ BMDCs transduced with TYF-RPE65 or the control TYF-LacZ virus via tail vein injection 7 and 28 days prior to sacrifice and organ harvest. Lung, spleen, and bone marrow were harvested immediately and incubated at 4°C overnight in 5 volumes of RNALater (Life Technologies). Up to 30 mg of tissue was homogenized in RLT Lysis Buffer (Qiagen), and mRNA was isolated as per directions for animal tissue using the Qiagen RNAEasy Mini Kit. Following isolation, mRNA was quantified (ThermoScientific NanoDrop 2000), and cDNA was synthesized from 1 μg RNA per sample as per directions using iScript Reverse-Transcription Supermix (BioRad). To quantify GFP expression in all tissues by qRT-PCR, 1 μL cDNA per sample was combined with 5 μL SsoFast Advanced (BioRad), 3.5 μL dH_2O, and 0.5 μL each of GFP forward (AAGCTGACCCTGAAGTTCATCTGC) and GFP reverse (CTTGT AGTTGCCGTCGTCCTTGAA) primers (10 μM stock; Integrated DNA Technologies), or 0.5 μL GAPDH primer (BioRad PrimePCR GAPDH, Mmu) as an internal control, and run on the BioRad CFX96 qRT-PCR machine as per manufacturer's directions (SsoFast Advanced, BioRad). GFP expression was calculated as fold of control

using the $2^{-\Delta\Delta CT}$ method. The sensitivity of this method is sufficient to detect as few as ten cells in a tissue sample.

Histological Analysis

Eyes were fixed with 4% paraformaldehyde (Wako) and embedded in paraffin, and 10-μm sections were stained with hematoxylin and eosin according to standard protocols. For histological sections, we view a complete cross-section of the retina, but measurements were taken between 0.2 and 1.2 mm adjacent to the optic nerve head. The thickness of the neural retina (from inner limiting layer to photoreceptor inner/outer segments) was evaluated as previously described.[20]

Immunofluorescence and Immunostaining

Retina and RPE/choroid flat mounts, and embedded sections, were deparaffinized and processed for antigen-epitope retrieval. Samples were incubated in a streamer autoclave at 120°C for 10 min in antigen retrieval solution (Histofine, Nichirei Biosciences) and then allowed to cool. Sections were then incubated with protein-blocking serum-free solution (Dako). For double staining, the anti-RPE65 and anti-CRALBP antibodies (Calbiochem) were added to the slides and incubated overnight at 4°C. We also stained additional sections with the following antibodies: anti-4 hydroxynonenal antibody (catalog #STA-035, Cell Biolabs), anti-rhodopsin antibody (catalog #ab3267, Abcam), and anti-ZO-1 antibody (catalog #40-2300, Thermo Fisher Scientific). After washing the slides the following day, the secondary antibodies Alexa Fluor-labeled (594 nm) and red goat anti-rabbit IgG (Molecular Probes) were added and incubated at room temperature for 1 hr. Slides were washed, and anti-fade reagent with DAPI (Prolong Gold antifade reagent with DAPI, Molecular Probes) was added. Pictures were taken within 24 hr using a fluorescence microscope (Leica). Confocal imaging was taken by using an Olympus Fluroview unit and an Olympus BX50 confocal microscope (Olympus).

Statistical Analysis

All experiments were repeated at least three times. Results are expressed as mean ± SEM. Unpaired two-tailed Student's t test and ANOVA with Bonferroni post hoc tests were carried out to determine significance of results in the ex vivo assay (Figure S1), in vivo assays, and all functional tests. Statistical analysis was performed using Prism 5 version 5.01 (GraphPad Software) with p values < 0.05 considered to indicate statistical significance.

SUPPLEMENTAL INFORMATION

Supplemental Information includes four figures and can be found with this article online at http://dx.doi.org/10.1016/j.ymthe.2017.01.015.

AUTHOR CONTRIBUTIONS

M.E.B. and M.B.G. conceived, designed, and supervised the study. M.E.B., M.B.G., and X.Q. interpreted the data and wrote the manuscript. L.-J.C. and S.L.P. generated the lentiviral vectors. X.Q. and S.L.P. performed the animal studies. A.S.L. and J.T. assisted with the SOD2-knockdown model. Y.Y. prepared the bone marrow cells and performed the statistical analyses.

ACKNOWLEDGMENTS

This research was supported by the NIH (EY023629), BrightFocus (M2009024), an unrestricted grant from Research to Prevent Blindness, and a National Eye Institute core grant to the University of Florida (P30 EY02172).

REFERENCES

1. Marquez-Curtis, L.A., Turner, A.R., Sridharan, S., Ratajczak, M.Z., and Janowska-Wieczorek, A. (2011). The ins and outs of hematopoietic stem cells: studies to improve transplantation outcomes. Stem Cell Rev. *7*, 590–607.
2. Treleaven, J., and Barrett, A.J. (2009). Hematopoietic Stem Cell Transplantation in Clinical Practice (Amsterdam: Churchill Livingstone Elsevier).
3. Dawn, B., and Bolli, R. (2005). Adult bone marrow-derived cells: regenerative potential, plasticity, and tissue commitment. Basic Res. Cardiol. *100*, 494–503.
4. Orlic, D., Kajstura, J., Chimenti, S., Jakoniuk, I., Anderson, S.M., Li, B., Pickel, J., McKay, R., Nadal-Ginard, B., Bodine, D.M., et al. (2001). Bone marrow cells regenerate infarcted myocardium. Nature *410*, 701–705.
5. Yoon, Y.S., Wecker, A., Heyd, L., Park, J.S., Tkebuchava, T., Kusano, K., Hanley, A., Scadova, H., Qin, G., Cha, D.H., et al. (2005). Clonally expanded novel multipotent stem cells from human bone marrow regenerate myocardium after myocardial infarction. J. Clin. Invest. *115*, 326–338.
6. Kucia, M., Dawn, B., Hunt, G., Guo, Y., Wysoczynski, M., Majka, M., Ratajczak, J., Rezzoug, F., Ildstad, S.T., Bolli, R., and Ratajczak, M.Z. (2004). Cells expressing early cardiac markers reside in the bone marrow and are mobilized into the peripheral blood after myocardial infarction. Circ. Res. *95*, 1191–1199.
7. Theise, N.D., Badve, S., Saxena, R., Henegariu, O., Sell, S., Crawford, J.M., and Krause, D.S. (2000). Derivation of hepatocytes from bone marrow cells in mice after radiation-induced myeloablation. Hepatology *31*, 235–240.
8. Theise, N.D., Nimmakayalu, M., Gardner, R., Illei, P.B., Morgan, G., Teperman, L., Henegariu, O., and Krause, D.S. (2000). Liver from bone marrow in humans. Hepatology *32*, 11–16.
9. El-Mahdi, M.M., Mansour, W.A., Hammam, O., Mehana, N.A., and Hussein, T.M. (2014). Ameliorative effect of bone marrow-derived stem cells on injured liver of mice infected with Schistosoma mansoni. Korean J. Parasitol. *52*, 151–162.
10. Iskovich, S., Goldenberg-Cohen, N., Stein, J., Yaniv, I., Fabian, I., and Askenasy, N. (2012). Elutriated stem cells derived from the adult bone marrow differentiate into insulin-producing cells in vivo and reverse chemical diabetes. Stem Cells Dev. *21*, 86–96.
11. Ratajczak, M.Z., Kucia, M., Reca, R., Majka, M., Janowska-Wieczorek, A., and Ratajczak, J. (2004). Stem cell plasticity revisited: CXCR4-positive cells expressing mRNA for early muscle, liver and neural cells 'hide out' in the bone marrow. Leukemia *18*, 29–40.
12. Kucia, M., Ratajczak, J., Reca, R., Janowska-Wieczorek, A., and Ratajczak, M.Z. (2004). Tissue-specific muscle, neural and liver stem/progenitor cells reside in the bone marrow, respond to an SDF-1 gradient and are mobilized into peripheral blood during stress and tissue injury. Blood Cells Mol. Dis. *32*, 52–57.
13. Eglitis, M.A., and Mezey, E. (1997). Hematopoietic cells differentiate into both microglia and macroglia in the brains of adult mice. Proc. Natl. Acad. Sci. U S A *94*, 4080–4085.
14. Okonogi, N., Nakamura, K., Suzuki, Y., Suto, N., Suzue, K., Kaminuma, T., Nakano, T., and Hirai, H. (2014). Cranial irradiation induces bone marrow-derived microglia in adult mouse brain tissue. J. Radiat. Res. (Tokyo) *55*, 713–719.
15. Mezey, E., Chandross, K.J., Harta, G., Maki, R.A., and McKercher, S.R. (2000). Turning blood into brain: cells bearing neuronal antigens generated in vivo from bone marrow. Science *290*, 1779–1782.
16. Atmaca-Sonmez, P., Li, Y., Yamauchi, Y., Schanie, C.L., Ildstad, S.T., Kaplan, H.J., and Enzmann, V. (2006). Systemically transferred hematopoietic stem cells home

to the subretinal space and express RPE-65 in a mouse model of retinal pigment epithelium damage. Exp. Eye Res. *83*, 1295–1302.

17. Chan-Ling, T., Baxter, L., Afzal, A., Sengupta, N., Caballero, S., Rosinova, E., and Grant, M.B. (2006). Hematopoietic stem cells provide repair functions after laser-induced Bruch's membrane rupture model of choroidal neovascularization. Am. J. Pathol. *168*, 1031–1044.
18. Grant, M.B., May, W.S., Caballero, S., Brown, G.A., Guthrie, S.M., Mames, R.N., Byrne, B.J., Vaught, T., Spoerri, P.E., Peck, A.B., and Scott, E.W. (2002). Adult hematopoietic stem cells provide functional hemangioblast activity during retinal neovascularization. Nat. Med. *8*, 607–612.
19. Harris, J.R., Brown, G.A., Jorgensen, M., Kaushal, S., Ellis, E.A., Grant, M.B., and Scott, E.W. (2006). Bone marrow-derived cells home to and regenerate retinal pigment epithelium after injury. Invest. Ophthalmol. Vis. Sci. *47*, 2108–2113.
20. Sengupta, N., Caballero, S., Sullivan, S.M., Chang, L.J., Afzal, A., Li Calzi, S., Kielczewski, J.L., Prabarakan, S., Ellis, E.A., Moldovan, L., et al. (2009). Regulation of adult hematopoietic stem cells fate for enhanced tissue-specific repair. Mol. Ther. *17*, 1594–1604.
21. van Lookeren Campagne, M., LeCouter, J., Yaspan, B.L., and Ye, W. (2014). Mechanisms of age-related macular degeneration and therapeutic opportunities. J. Pathol. *232*, 151–164.
22. Justilien, V., Pang, J.J., Renganathan, K., Zhan, X., Crabb, J.W., Kim, S.R., Sparrow, J.R., Hauswirth, W.W., and Lewin, A.S. (2007). SOD2 knockdown mouse model of early AMD. Invest. Ophthalmol. Vis. Sci. *48*, 4407–4420.
23. Seo, S.J., Krebs, M.P., Mao, H., Jones, K., Conners, M., and Lewin, A.S. (2012). Pathological consequences of long-term mitochondrial oxidative stress in the mouse retinal pigment epithelium. Exp. Eye Res. *101*, 60–71.
24. Beatty, S., Koh, H., Phil, M., Henson, D., and Boulton, M. (2000). The role of oxidative stress in the pathogenesis of age-related macular degeneration. Surv. Ophthalmol. *45*, 115–134.
25. de Jong, P.T. (2006). Age-related macular degeneration. N. Engl. J. Med. *355*, 1474–1485.
26. Boulton, M.E. (2016). Lipofuscin of the retinal pigment epithelium. In Fundus Autofluorescence, Second Edition, N. Lois and J.V. Forrester, eds. (Philadelphia: Wolters Kluwer), pp. 3–13.
27. Thampi, P., Rao, H.V., Mitter, S.K., Cai, J., Mao, H., Li, H., Seo, S., Qi, X., Lewin, A.S., Romano, C., and Boulton, M.E. (2012). The 5HT1a receptor agonist 8-Oh DPAT induces protection from lipofuscin accumulation and oxidative stress in the retinal pigment epithelium. PLoS ONE *7*, e34468.
28. Combadière, C., Feumi, C., Raoul, W., Keller, N., Rodéro, M., Pézard, A., Lavalette, S., Houssier, M., Jonet, L., Picard, E., et al. (2007). CX3CR1-dependent subretinal microglia cell accumulation is associated with cardinal features of age-related macular degeneration. J. Clin. Invest. *117*, 2920–2928.
29. Cai, J., Qi, X., Kociok, N., Skosyrski, S., Emilio, A., Ruan, Q., Han, S., Liu, L., Chen, Z., Bowes Rickman, C., et al. (2012). β-Secretase (BACE1) inhibition causes retinal pathology by vascular dysregulation and accumulation of age pigment. EMBO Mol. Med. *4*, 980–991.
30. Friedman, D.S., O'Colmain, B.J., Muñoz, B., Tomany, S.C., McCarty, C., de Jong, P.T., Nemesure, B., Mitchell, P., and Kempen, J.; Eye Diseases Prevalence Research Group (2004). Prevalence of age-related macular degeneration in the United States. Arch. Ophthalmol. *122*, 564–572.
31. Binder, S., Stanzel, B.V., Krebs, I., and Glittenberg, C. (2007). Transplantation of the RPE in AMD. Prog. Retin. Eye Res. *26*, 516–554.
32. da Cruz, L., Chen, F.K., Ahmado, A., Greenwood, J., and Coffey, P. (2007). RPE transplantation and its role in retinal disease. Prog. Retin. Eye Res. *26*, 598–635.
33. Rowland, T.J., Buchholz, D.E., and Clegg, D.O. (2012). Pluripotent human stem cells for the treatment of retinal disease. J. Cell. Physiol. *227*, 457–466.
34. Boulton, M.E. (2004). [RPE transplantation: the challenges and the future]. Ophthalmologe *101*, 877–881.
35. Vugler, A., Carr, A.J., Lawrence, J., Chen, L.L., Burrell, K., Wright, A., Lundh, P., Semo, M., Ahmado, A., Gias, C., et al. (2008). Elucidating the phenomenon of HESC-derived RPE: anatomy of cell genesis, expansion and retinal transplantation. Exp. Neurol. *214*, 347–361.
36. Du, H., Lim, S.L., Grob, S., and Zhang, K. (2011). Induced pluripotent stem cell therapies for geographic atrophy of age-related macular degeneration. Semin. Ophthalmol. *26*, 216–224.
37. Bazan, N.G. (2008). Neurotrophins induce neuroprotective signaling in the retinal pigment epithelial cell by activating the synthesis of the anti-inflammatory and anti-apoptotic neuroprotectin D1. Adv. Exp. Med. Biol. *613*, 39–44.
38. Tombran-Tink, J., and Barnstable, C.J. (2003). PEDF: a multifaceted neurotrophic factor. Nat. Rev. Neurosci. *4*, 628–636.
39. Nygren, J.M., Jovinge, S., Breitbach, M., Säwén, P., Röll, W., Hescheler, J., Taneera, J., Fleischmann, B.K., and Jacobsen, S.E. (2004). Bone marrow-derived hematopoietic cells generate cardiomyocytes at a low frequency through cell fusion, but not transdifferentiation. Nat. Med. *10*, 494–501.
40. Spees, J.L., Olson, S.D., Ylostalo, J., Lynch, P.J., Smith, J., Perry, A., Peister, A., Wang, M.Y., and Prockop, D.J. (2003). Differentiation, cell fusion, and nuclear fusion during ex vivo repair of epithelium by human adult stem cells from bone marrow stroma. Proc. Natl. Acad. Sci. U S A *100*, 2397–2402.
41. Alvarez-Dolado, M., Pardal, R., Garcia-Verdugo, J.M., Fike, J.R., Lee, H.O., Pfeffer, K., Lois, C., Morrison, S.J., and Alvarez-Buylla, A. (2003). Fusion of bone-marrow-derived cells with Purkinje neurons, cardiomyocytes and hepatocytes. Nature *425*, 968–973.
42. Wang, X., Willenbring, H., Akkari, Y., Torimaru, Y., Foster, M., Al-Dhalimy, M., Lagasse, E., Finegold, M., Olson, S., and Grompe, M. (2003). Cell fusion is the principal source of bone-marrow-derived hepatocytes. Nature *422*, 897–901.
43. Vassilopoulos, G., and Russell, D.W. (2003). Cell fusion: an alternative to stem cell plasticity and its therapeutic implications. Curr. Opin. Genet. Dev. *13*, 480–485.
44. Vassilopoulos, G., Wang, P.R., and Russell, D.W. (2003). Transplanted bone marrow regenerates liver by cell fusion. Nature *422*, 901–904.
45. Bae, J.S., Furuya, S., Shinoda, Y., Endo, S., Schuchman, E.H., Hirabayashi, Y., and Jin, H.K. (2005). Neurodegeneration augments the ability of bone marrow-derived mesenchymal stem cells to fuse with Purkinje neurons in Niemann-Pick type C mice. Hum. Gene Ther. *16*, 1006–1011.
46. Howell, J.C., Lee, W.H., Morrison, P., Zhong, J., Yoder, M.C., and Srour, E.F. (2003). Pluripotent stem cells identified in multiple murine tissues. Ann. N Y Acad. Sci. *996*, 158–173.
47. Avots, A., Harder, F., Schmittwolf, C., Petrovic, S., and Müller, A.M. (2002). Plasticity of hematopoietic stem cells and cellular memory. Immunol. Rev. *187*, 9–21.
48. Davies, V.J., Hollins, A.J., Piechota, M.J., Yip, W., Davies, J.R., White, K.E., Nicols, P.P., Boulton, M.E., and Votruba, M. (2007). Opa1 deficiency in a mouse model of autosomal dominant optic atrophy impairs mitochondrial morphology, optic nerve structure and visual function. Hum. Mol. Genet. *16*, 1307–1318.